STATISTICS, OPTIMIZATION AND INFORMATION COMPUTING
Stat., Optim. Inf. Comput., Vol. **14**, December 2025, pp 3418–3435.
Published online in International Academic Press (www.IAPress.org)

Exploring Nonlinear Reaction Kinetics in Porous Catalysts: Analytical and Numerical Approaches to LHHW Model

Regunathan Rajalakshmi [1], Lakshmanan Rajendran [2], Sethu Naganathan [3,*]

[1]*Department of Mathematics, Government Arts College for Women, Ramanathapuram-623501*
[2]*Department of Mathematics, AMET Deemed to be University, Kanathur, Chennai 603112*
[3]*Department of Mathematics, Sethupathy Government Arts College, Ramanthapuram-623502*

Abstract This article develops a mathematical model for porous catalysts with nonlinear reaction kinetics, governed by a steady-state reaction–diffusion equation. Using the Taylor series method, analytical solutions for species concentration in Langmuir–Hinshelwood–Hougen–Watson (LHHW) models are derived, yielding polynomial approximations for concentration and effectiveness factors. Comparisons with numerical simulations confirm strong agreement. The findings offer valuable guidance for optimizing catalytic and biochemical systems—such as reactors, fuel cells, and converters—promoting sustainable production, wastewater treatment, and energy applications, while minimizing trial-and-error methods and enabling efficient, cost-effective scale-up.

Keywords Mathematical modelling, Nonlinear equations, Taylor series method, Porous Catalysts, Numerical method

AMS 2010 subject classifications 35K57, 35G25

DOI: 10.19139/soic-2310-5070-2976

1. Introduction

Mass transfer limitations significantly influence reaction rates, conversion efficiency, and product formation, particularly in catalytic systems. In a homogeneous catalytic reaction, where reactants, products, and catalysts exist in the same phase, the impact of mass transfer is generally minor. Conversely, in heterogeneous catalytic reactions, the catalyst often occupies a different phase, typically solid, while the reactants are in liquid or gas phases. Therefore, the reaction rate strongly depends on the mass transfer or diffusion between the involved phases. Mass transfer limitations occur due to external diffusion from the fluid to the catalyst surface and intraparticle movement through the porous matrix. The mass transfer coefficient plays a crucial role in determining external transport rates. The Thiele modulus quantifies internal diffusion resistance by integrating the effects of effective diffusivity, reaction kinetics, and catalyst geometry, customized to fit the chosen kinetic model. The assortment of porous catalysts includes pellet forms (e.g., cylindrical, spherical, or Raschig ring shapes) and structured types such as washcoated monoliths used in advanced applications. Both systems experience internal mass transfer restrictions primarily due to the reaction rate dynamics. Diffusion processes in washcoats have been widely studied, with Leung et al. [1] and Hayes and Kolaczkowski [2] emphasizing simulations based on realistic structural models. They have introduced methods for effectively mapping these geometries onto different models. While some works have shown LHHW (Langmuir–Hinshelwood–Haugen–Watson) behaviour and proposed methods [3, 4] for estimating effectiveness factors in various washcoat thicknesses, no comprehensive analytical results for concentration and

*Correspondence to: Sethu Naganathan (Email: nathanaga@gmail.com). Department of Mathematics, Sethupathy Government Arts College, Ramanthapuram-623502.

ISSN 2310-5070 (online) ISSN 2311-004X (print)

effectiveness factors across all parameters have been established. This communication aims to provide a closed-form analytical expression for the concentration of reactants and effectiveness factors using the Taylor series method.

2. Mathematical Formulation

Mass transport phenomena in heterogeneous catalysts can be modeled using the general nonlinear reaction-diffusion equation, as shown in [5, 6].

$$(D_{\text{eff}})_A \frac{d^2C_A}{dX^2} - \frac{k_v C_A^p}{(1+K_A C_A)^m} = 0. \tag{1}$$

Where C_A (mol/m^3) and D_{eff} (m^2/s) are the molar concentration and effective diffusion coefficient of species A, respectively. k_v (mol^{p-1} m$^{-3(p-1)}$ s^{-1}) is the reaction rate constant, and K_A (m^3/mol) is the rate parameter for adsorption inhibition of species A. The constants $p = 1$ or 2, and $m = 2$ or 3 are numerical values. The boundary conditions are:

$$\left.\frac{dC_A}{dX}\right|_{x=0} = 0 \tag{2a}$$

$$C_A = (C_A)_s \quad \text{at} \quad x = l \tag{2b}$$

Where $(C_A)_s$ (mol/m^3) is the concentration at the external surface of the catalyst, and l (m) is the thickness of the flat plate catalyst. The dimensionless variables are introduced as follows:

$$c = \frac{C_A}{(C_A)_s}, \quad x = \frac{X}{l}, \quad \varphi = L_C\sqrt{\frac{k_v (C_s)^{p-1}}{D_{\text{eff}}}}, \quad \alpha = (C_A)_s K_A \tag{3}$$

The dimensionless parameter φ, known as the Thiele modulus, is defined for three geometries using a characteristic length, which is the ratio of particle volume to surface area. The characteristic length L_C (m) is given as: Sphere: $L_C = \frac{R}{3}$, Infinite Cylinder: $L_C = \frac{R}{2}$ Flat Plate: $L_C = l$.

where R (m) is the radius and l is the thickness of the plate.

(1) - (3) are reduced in the following dimensionless form.

$$\frac{d^2c(x)}{dx^2} - p\frac{dc(x)}{dx} - B(c(x)) = 0, \quad 0 \le x \le 1 \tag{4}$$

$$B(c) = \frac{\varphi^2[c(x)]^n}{[1+\alpha c(x)]^m}$$

$$\left.\frac{dc(x)}{dx}\right|_{x=0} = 0 \tag{5a}$$

$$c(1) = 1. \tag{5b}$$

The dimensionless effectiveness factor is

$$\eta = \frac{1+\alpha}{\varphi^2}\left(\frac{dc}{dx}\right)_{x=1} \tag{6}$$

Here, $c(x)$ represents the dimensionless concentration and x denotes the dimensionless distance. The parameters p, m, and n are dimensionless constants, while φ is the Thiele modulus, and α is another dimensionless parameter. The effectiveness factor is represented by η, which indicates the overall efficiency of the catalytic process.

3. Analytical expression of concentration c(x) and effectiveness factor

The Taylor series method demands lower computational resources and provides a more straightforward implementation for complex nonlinear models, including the LHHW-type kinetics investigated in this work. Unlike the Homotopy analysis method (HAM), Homotopy Perturbation Method (HPM), or Differential transform method (DTM), which often require auxiliary parameters (e.g., convergence-control parameters in HAM or perturbation terms in HPM), TSM does not rely on such constructs. As a result, TSM requires less computational effort and offers easy implementation for highly nonlinear models, such as LHHW-type kinetics explored in this study. The nonlinear equation explored in this paper includes reaction-diffusion terms with complex kinetics, where the reaction rates depend on arbitrary exponents m and n, along with a parameter p. These characteristics often hinder the convergence and stability of traditional techniques such as HAM and HPM. However, the Taylor Series Method (TSM) proved effective, generating quickly converging polynomial solutions for the concentration profiles. The excellent consistency with numerical results, along with its computational speed, supports the suitability of TSM for this application. The analytical solution of nonlinear equations is crucial due to its broad applications in scientific research. The Taylor Series Method (TSM) has emerged as a preferred method among many authors [7, 8, 9] due to its accuracy and versatility in solving nonlinear models in applied mathematics [10, 11, 12, 13]. The basic concept of TSM is given in Appendix A. Solving (4) using TSM, we can obtain the concentration as follows: The approximate analytical expression of concentration has suggested the Taylor series method.

$$c(x) = k + \frac{\varphi^2 k^n}{[1+\alpha k]^m}\left(\frac{x^2}{2!} + \frac{px^3}{3!} + \frac{p^2x^4}{4!} + \frac{p^3x^5}{5!}\right) \tag{7}$$

Using (6), we can obtain the effectiveness factor as,

$$\eta = \left(\frac{(1+\alpha)\,k^n}{(1+\alpha k)^m}\right)\left(1 + \frac{p}{2} + \frac{p^2}{6} + \frac{p^3}{24}\right) \tag{8}$$

(7) and (8) represent the general analytical expressions for the concentration and effectiveness factor for arbitrary values of p, n, and m. The complete derivation of the concentration expression is provided in Appendix A.

4. Numerical Simulations

The differential (4) with the boundary conditions (5a) and (5b) has been solved numerically using MATLAB software. The numerical solution is compared with our analytical results in Tables 1–5 and Figs. 1–5. The analytical and numerical results demonstrate a satisfactory agreement. The limitations encountered while using MATLAB for solving the nonlinear reaction-diffusion equations are noteworthy. The equations became stiff for large values of the Thiele modulus (φ) or in the presence of higher-order nonlinearities involving parameters such as m, n, and p, necessitating the use of advanced solvers with finely tuned tolerance settings to ensure numerical stability and convergence. The numerical method exhibited sensitivity to boundary conditions, especially when determining the unknown constant k for the Taylor series approach. Wolfram Alpha was employed to perform symbolic calculations and to verify the constants obtained from the boundary conditions, ensuring accuracy in the solution process. While MATLAB handled simulations efficiently for moderate parameter ranges, computational time increased significantly with finer mesh resolutions or during extensive parameter sensitivity analyses. Nonetheless, the numerical results showed excellent agreement with the analytical Taylor series solutions, with deviations typically below 0.01, confirming the robustness of the numerical approach.

5. Results and Discussion

Mathematical models that involve multiple variables for different processes lead to the formation of nonlinear differential equations. Here, we can apply the Taylor series method (TSM) [6].to solve the nonlinear (4). TSM's advantages in solving complex nonlinear differential equations are its simplicity and effectiveness compared to earlier methods. The nonlinear differential (4) was solved using MATLAB, a numerical software. The analytical solution (4) was compared with the numerical results in Tables (1)–(5) and Figs. (1)–(5) for various experimental values of parameters. The new analytical and simulated results are very close. In addition, the relative average deviation is less than 0.05.

Table 1. Comparison between the numerical and analytical results for the concentration $c(x)$ for various values of φ for $p = 0, n = 1, m = 2, \alpha = 45$.

x	**Numerical**					**TSM Eq. 7**					**Deviation**				
	$\varphi = 5$	$\varphi = 10$	$\varphi = 15$	$\varphi = 20$	$\varphi = 25$	$\varphi = 5$	$\varphi = 10$	$\varphi = 15$	$\varphi = 20$	$\varphi = 25$	$\varphi = 5$	$\varphi = 10$	$\varphi = 15$	$\varphi = 20$	$\varphi = 25$
						$k = 0.9941$	$k = 0.9758$	$k = 0.9438$	$k = 0.8949$	$k = 0.8220$					
0.0	0.9941	0.9759	0.9444	0.8970	0.8289	0.9941	0.9758	0.9438	0.8949	0.8220	0.0000	0.0001	0.0006	0.0021	0.0069
0.1	0.9941	0.9762	0.9449	0.8981	0.8307	0.9941	0.9761	0.9444	0.8960	0.8238	0.0000	0.0001	0.0005	0.0021	0.0069
0.2	0.9943	0.9769	0.9467	0.9013	0.8361	0.9943	0.9768	0.9461	0.8992	0.8293	0.0000	0.0001	0.0006	0.0021	0.0068
0.3	0.9946	0.9781	0.9495	0.9066	0.8450	0.9946	0.9780	0.9490	0.9048	0.8384	0.0000	0.0001	0.0005	0.0018	0.0066
0.4	0.9950	0.9799	0.9535	0.9141	0.8575	0.9950	0.9798	0.9530	0.9121	0.8511	0.0000	0.0001	0.0005	0.0020	0.0064
0.5	0.9956	0.9821	0.9587	0.9236	0.8735	0.9956	0.9820	0.9582	0.9217	0.8674	0.0000	0.0001	0.0005	0.0019	0.0061
0.6	0.9963	0.9848	0.9649	0.9353	0.8930	0.9962	0.9847	0.9645	0.9335	0.8874	0.0001	0.0001	0.0004	0.0018	0.0056
0.7	0.9970	0.9880	0.9723	0.9490	0.9157	0.9970	0.9879	0.9719	0.9475	0.9110	0.0000	0.0001	0.0004	0.0015	0.0047
0.8	0.9979	0.9917	0.9808	0.9647	0.9418	0.9979	0.9916	0.9805	0.9635	0.9382	0.0000	0.0001	0.0003	0.0012	0.0036
0.9	0.9990	0.9958	0.9904	0.9824	0.9710	0.9990	0.9958	0.9903	0.9818	0.9691	0.0000	0.0000	0.0001	0.0006	0.0019
1.0	1.0000	1.0000	1.0000	1.0000	1.0000	1.0000	1.0000	1.0000	1.0000	1.0000	0.0000	0.0000	0.0000	0.0000	0.0000
Average Deviation											**0.0000**	**0.0001**	**0.0004**	**0.0016**	**0.0050**

Table 2. Comparison between the numerical and analytical results for the concentration $c(x)$ for various values of α for $p = 0, m = 2, n = 1, \varphi = 2$.

x	**Numerical**					**TSM Eq. 7**					**Deviation**				
	$\alpha = 0.5$	$\alpha = 1$	$\alpha = 1.5$	$\alpha = 2$	$\alpha = 10$	$\alpha = 0.5$	$\alpha = 1$	$\alpha = 1.5$	$\alpha = 2$	$\alpha = 10$	$\alpha = 0.5$	$\alpha = 1$	$\alpha = 1.5$	$\alpha = 2$	$\alpha = 10$
						$k = 0.4233$	$k = 0.5437$	$k = 0.6667$	$k = 0.7607$	$k = 0.9832$					
0.0	0.3846	0.5325	0.6678	0.7636	0.8677	0.4233	0.5437	0.6667	0.8662	0.9832	0.0387	0.0112	0.0011	0.0029	0.0015
0.1	0.3901	0.5372	0.6712	0.7660	0.8690	0.4292	0.5483	0.6701	0.8676	0.9834	0.0391	0.0111	0.0011	0.0033	0.0014
0.2	0.4068	0.5511	0.6814	0.7734	0.8731	0.4469	0.5623	0.6803	0.8717	0.9839	0.0410	0.0112	0.0011	0.0017	0.0008
0.3	0.4350	0.5743	0.6984	0.7855	0.8799	0.4763	0.5856	0.6973	0.8785	0.9843	0.0413	0.0113	0.0011	0.0070	0.0004
0.4	0.4752	0.6071	0.7222	0.8026	0.8895	0.5175	0.6182	0.7211	0.8881	0.9860	0.0423	0.0111	0.0011	0.0028	0.0032
0.5	0.5280	0.6494	0.7528	0.8244	0.9017	0.5704	0.6601	0.7517	0.8975	0.9874	0.0424	0.0107	0.0012	0.0029	0.0043
0.6	0.5944	0.7014	0.7901	0.8511	0.9166	0.6351	0.7113	0.7891	0.9145	0.9894	0.0407	0.0099	0.0010	0.0034	0.0078
0.7	0.6752	0.7634	0.8342	0.8825	0.9342	0.7116	0.7718	0.8333	0.9333	0.9916	0.0364	0.0084	0.0009	0.0008	0.0057
0.8	0.7713	0.8353	0.8351	0.9186	0.9544	0.7999	0.8417	0.8438	0.9536	0.9942	0.0286	0.0064	0.0006	0.0030	0.0032
0.9	0.8339	0.9174	0.9426	0.9594	0.9773	0.8992	0.9242	0.9585	0.9768	0.9971	0.0653	0.0068	0.0159	0.0174	0.0010
1.0	1.0000	1.0000	1.0000	1.0000	1.0000	1.0000	1.0000	1.0000	1.0000	1.0000	0.0000	0.0000	0.0000	0.0000	0.0000
Average Deviation											**0.0332**	**0.0086**	**0.0009**	**0.0022**	**0.0011**

Table 3. Comparison between the numerical and analytical results for the concentration $c(x)$ for various values of m for $p = 0$, $\alpha = 10$, $n = 1$, $\varphi = 2$.

x	**Numerical**					**TSM Eq. 7**					**Deviation**				
	$m = 0.5$	$m = 0.8$	$m = 1$	$m = 1.5$	$m = 3$	$m = 0.5$	$m = 0.8$	$m = 1$	$m = 1.5$	$m = 3$	$m = 0.5$	$m = 0.8$	$m = 1$	$m = 1.5$	$m = 3$
						$k = 0.5628$	$k = 0.7313$	$k = 0.8217$	$k = 0.9440$	$k = 0.9985$					
0.0	0.5412	0.7269	0.8209	0.9442	0.9985	0.5628	0.7313	0.8217	0.9440	0.9985	0.0216	0.0044	0.0008	0.0002	0.0000
0.1	0.5457	0.7296	0.8228	0.9448	0.9985	0.5673	0.7340	0.8235	0.9446	0.9985	0.0216	0.0044	0.0007	0.0002	0.0001
0.2	0.5588	0.7378	0.8282	0.9465	0.9986	0.5806	0.7422	0.8290	0.9463	0.9986	0.0218	0.0044	0.0008	0.0002	0.0000
0.3	0.5808	0.7516	0.8373	0.9494	0.9986	0.6029	0.7560	0.8381	0.9492	0.9986	0.0221	0.0044	0.0008	0.0002	0.0000
0.4	0.6120	0.7708	0.8501	0.9534	0.9987	0.6342	0.7751	0.8508	0.9532	0.9987	0.0222	0.0043	0.0007	0.0002	0.0000
0.5	0.6525	0.7957	0.8665	0.9585	0.9989	0.6743	0.7998	0.8672	0.9583	0.9989	0.0218	0.0041	0.0007	0.0002	0.0000
0.6	0.7027	0.8262	0.8866	0.9648	0.9991	0.7234	0.8300	0.8872	0.9646	0.9991	0.0207	0.0038	0.0006	0.0002	0.0000
0.7	0.7631	0.8623	0.9103	0.9722	0.9993	0.7814	0.8656	0.9108	0.9720	0.9993	0.0183	0.0033	0.0005	0.0002	0.0000
0.8	0.8340	0.9042	0.9377	0.9807	0.9995	0.8483	0.9068	0.9381	0.9806	0.9995	0.0143	0.0026	0.0004	0.0001	0.0000
0.9	0.9161	0.9520	0.9688	0.9904	0.9997	0.9241	0.9534	0.9691	0.9903	0.9997	0.0080	0.0014	0.0003	0.0001	0.0000
1.0	1.0000	1.0000	1.0000	1.0000	1.0000	1.0000	1.0000	1.0000	1.0000	1.0000	0.0000	0.0000	0.0000	0.0000	0.0000
Average Deviation											**0.0175**	**0.0034**	**0.0006**	**0.0002**	**0.0000**

Table 4. Comparison between the numerical and analytical results for the concentration $c(x)$ for various values of n for $p = 0$, $\alpha = 0.1$, $m = 2$, $\varphi = 1$.

x	**Numerical**					**TSM Eq. 7**					**Deviation**				
	$n = 0$	$n = 0.5$	$n = 1.5$	$n = 5$	$n = 20$	$n = 0$	$n = 0.5$	$n = 1.5$	$n = 5$	$n = 20$	$n = 0$	$n = 0.5$	$n = 1.5$	$n = 5$	$n = 20$
						$k = 0.5509$	$k = 0.6455$	$k = 0.7294$	$k = 0.8310$	$k = 0.9203$					
0.0	0.5576	0.6361	0.7140	0.8158	0.9107	0.5509	0.6455	0.7294	0.8310	0.9203	0.0067	0.0094	0.0154	0.0152	0.0096
0.1	0.5622	0.6397	0.7167	0.8174	0.9114	0.5554	0.6491	0.7322	0.8328	0.9211	0.0068	0.0094	0.0155	0.0154	0.0097
0.2	0.5759	0.6505	0.7247	0.8222	0.9134	0.5692	0.6600	0.7405	0.8379	0.9236	0.0067	0.0095	0.0158	0.0157	0.0102
0.3	0.5987	0.6686	0.7383	0.8302	0.9168	0.5921	0.6781	0.7543	0.8466	0.9276	0.0066	0.0095	0.0160	0.0164	0.0108
0.4	0.6307	0.6940	0.7575	0.8417	0.9217	0.6242	0.7034	0.7708	0.8586	0.9333	0.0065	0.0094	0.0161	0.0169	0.0116
0.5	0.6716	0.7268	0.7825	0.8568	0.9283	0.6654	0.7359	0.7984	0.8741	0.9407	0.0062	0.0091	0.0159	0.0173	0.0124
0.6	0.7215	0.7671	0.8135	0.8760	0.9368	0.7158	0.7757	0.8288	0.8931	0.9496	0.0057	0.0086	0.0153	0.0171	0.0128
0.7	0.7803	0.8153	0.8510	0.8996	0.9477	0.7754	0.8227	0.8647	0.9155	0.9602	0.0049	0.0074	0.0137	0.0159	0.0125
0.8	0.8479	0.8713	0.8953	0.9283	0.9615	0.8441	0.8770	0.9061	0.9414	0.9724	0.0038	0.0057	0.0108	0.0131	0.0109
0.9	0.9241	0.9353	0.9469	0.9629	0.9793	0.9221	0.9385	0.9530	0.9707	0.9862	0.0020	0.0032	0.0061	0.0078	0.0069
1.0	1.0000	1.0000	1.0000	1.0000	1.0000	1.0000	1.0000	1.0000	1.0000	1.0000	0.0000	0.0000	0.0000	0.0000	0.0000
Average Deviation											**0.0051**	**0.0074**	**0.0128**	**0.0137**	**0.0098**

Table 5. Comparison between the numerical and analytical results for the concentration $c(x)$ for various values of p for $n = 1$, $\alpha = 3.5$, $m = 2$, $\varphi = 3$.

x	**Numerical**					**TSM Eq. 7**					**Deviation**				
	$p = 0$	$p = 1$	$p = 1.5$	$p = 2$	$p = 3$	$p = 0$	$p = 1$	$p = 1.5$	$p = 2$	$p = 3$	$p = 0$	$p = 1$	$p = 1.5$	$p = 2$	$p = 3$
						$k = 0.7419$	$k = 0.5964$	$k = 0.4817$	$k = 0.3160$	$k = 0.1261$					
0.0	0.7493	0.6100	0.4866	0.3104	0.0863	0.7419	0.5964	0.4817	0.3160	0.1261	0.0074	0.0136	0.0049	0.0056	0.0398
0.1	0.7519	0.6129	0.4899	0.3139	0.0889	0.7446	0.5994	0.4849	0.3195	0.1292	0.0073	0.0135	0.0050	0.0056	0.0403
0.2	0.7598	0.6222	0.5002	0.3254	0.0979	0.7525	0.6088	0.4953	0.3311	0.1398	0.0073	0.0134	0.0049	0.0057	0.0419
0.3	0.7729	0.6384	0.5188	0.3468	0.1161	0.7656	0.6251	0.5140	0.3524	0.1606	0.0073	0.0133	0.0048	0.0056	0.0445
0.4	0.7911	0.6622	0.5470	0.3801	0.1469	0.7841	0.6493	0.5423	0.3855	0.1946	0.0070	0.0129	0.0047	0.0054	0.0477
0.5	0.8144	0.6943	0.5862	0.4280	0.1955	0.8078	0.6820	0.5817	0.4330	0.2456	0.0066	0.0123	0.0045	0.0050	0.0501
0.6	0.8428	0.7356	0.6380	0.4937	0.2686	0.8367	0.7243	0.6340	0.4975	0.3182	0.0061	0.0113	0.0040	0.0038	0.0496
0.7	0.8762	0.7868	0.7043	0.5807	0.3753	0.8710	0.7771	0.7011	0.5824	0.4176	0.0052	0.0097	0.0032	0.0017	0.0423
0.8	0.9144	0.8488	0.7873	0.6937	0.5270	0.9104	0.8414	0.7851	0.6911	0.5500	0.0040	0.0074	0.0022	0.0026	0.0230
0.9	0.9574	0.9226	0.8894	0.8380	0.7397	0.9552	0.9186	0.8868	0.8279	0.7223	0.0022	0.0040	0.0026	0.0100	0.0174
1.0	1.0000	1.0000	1.0000	1.0000	1.0000	1.0000	1.0000	1.0000	1.0000	1.0000	0.0000	0.0000	0.0000	0.0000	0.0000
Average Deviation											**0.0055**	**0.0101**	**0.0036**	**0.0046**	**0.0361**

5.1. Impact of the parameters on c(x)

To understand the dynamics of substrate diffusion and reaction within the system, a parametric analysis is performed by examining the effect of various dimensionless parameters on the concentration profile $c(x)$. This analysis helps identify how changes in reaction kinetics, transport properties, and saturation behavior influence the distribution of the substrate across the spatial domain. The parameters considered include the Thiele modulus φ, the saturation constant α, the kinetic exponent m, the reaction order n, and the advection-related parameter p. By varying each parameter independently while keeping others constant, the sensitivity of the model is analyzed and visualized. Figure (1)-(5) shows the comparative effects of these parameters, as described below.

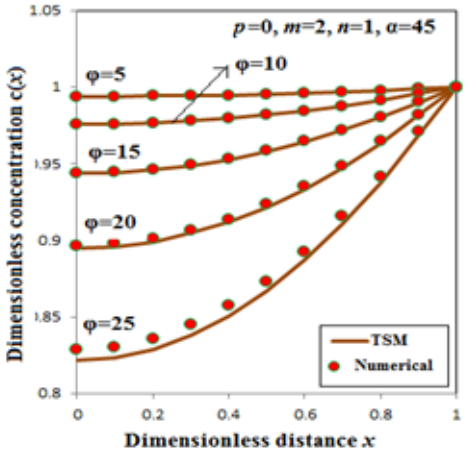

Figure 1. Dimensionless concentration profiles $c(x)$ as a function of dimensionless distance x for various Thiele modulus values ($\varphi = 5, 10, 15, 20, 25$) are compared between the Taylor Series Method (TSM) and numerical results for $p = 0$, $m = 2$, $n = 1$, and $\alpha = 45$.

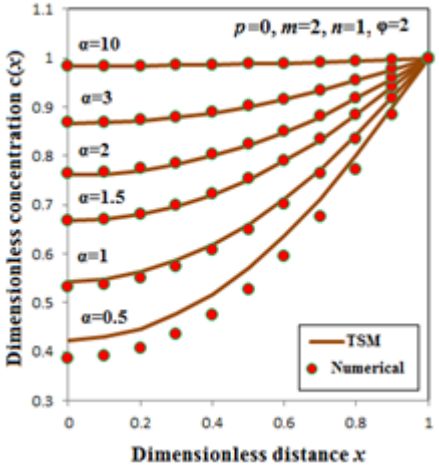

Figure 2. Dimensionless concentration profiles $c(x)$ as a function of dimensionless distance x for various values of the parameter α ($\alpha = 0.5, 1, 1.5, 2, 3, 10$) are compared between the Taylor Series Method (TSM) and numerical results for $p = 0,\ m = 2,\ n = 1,\ \varphi = 2$.

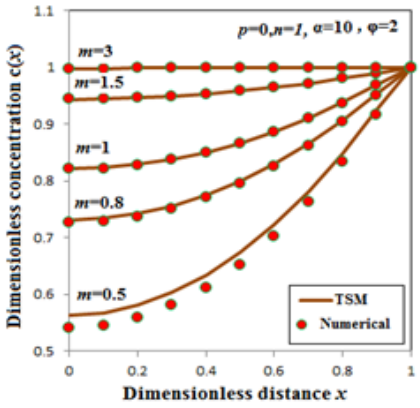

Figure 3. Dimensionless concentration profiles $c(x)$ as a function of dimensionless distance x for various values of the parameter m ($m = 0.5, 0.8, 1, 1.5, 3$) are compared between the Taylor Series Method (TSM) and numerical results for $p = 0,\ n = 1,\ \alpha = 10,\ \varphi = 2$.

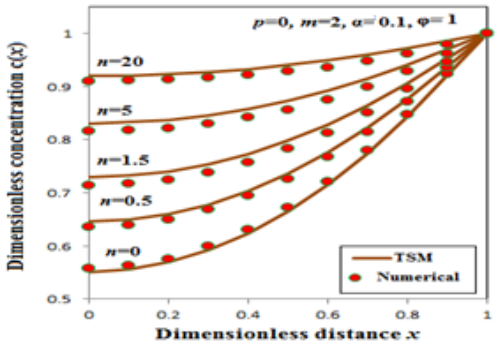

Figure 4. Dimensionless concentration profiles $c(x)$ as a function of dimensionless distance x for various values of the parameter n ($n = 0, 0.5, 1.5, 5, 20$) are compared between the Taylor Series Method (TSM) and numerical results for $p = 0$, $m = 2$, $\alpha = 0.1$, and $\phi = 1$.

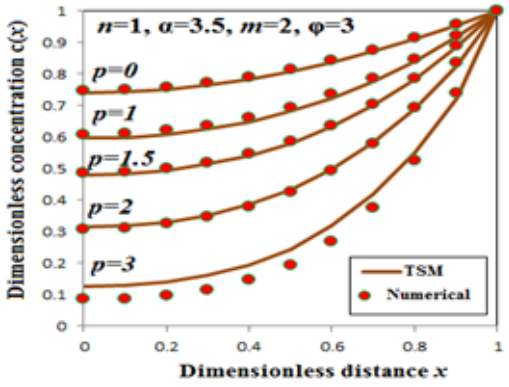

Figure 5. Dimensionless concentration profiles $c(x)$ as a function of dimensionless distance x for various values of the parameter p ($p = 0, 1, 1.5, 2, 3$) are compared between the Taylor Series Method (TSM) and numerical results for for n = 1, α = 3.5, m = 2, φ = 3.

5.1.1. Effect of φ on the concentration Figure (1) presents a comparison between the analytical (TSM) and numerical results for the dimensionless concentration $c(x)$ as a function of dimensionless distance x for various values of the Thiele modulus φ (5, 10, 15, 20, and 25). The parameters used are $p = 0$, $m = 2$, $n = 1$, and $\alpha = 45$. The graph demonstrates excellent agreement between the TSM and numerical results across all values of φ, validating the accuracy of the analytical solution. As it φ increases, the concentration profile becomes more nonlinear, indicating greater diffusion resistance within the system. This behaviour reflects the critical role φ in controlling mass transport in catalytic systems.

5.1.2. Effect of α on the concentration The influence of the kinetic parameter α on the concentration profile $c(x)$ is illustrated in Figure (2) for a fixed set of parameters: $p = 0$, $m = 2$, $n = 1$, and $\varphi = 2$. The comparison between the Taylor Series Method (TSM) and numerical results shows excellent agreement across all α values, confirming the accuracy of the analytical approach. As α increases from 0.5 to 10, the concentration $c(x)$ increases, indicating a reduced reaction rate and weaker nonlinear effects. This trend highlights the role of α in moderating substrate consumption and influencing mass transfer resistance in catalytic systems.

5.1.3. Effect of m on the concentration The impact of different values of the exponent m on the concentration distribution $c(x)$ is depicted by Figure (3), with parameters $p = 0$, $n = 1$, $\alpha = 10$, and $\varphi = 2$ held fixed. The figure compares the results of the Taylor Series Method (TSM) with numerical solutions, showing excellent agreement across all m values. As m increases from 0.5 to 3, the concentration $c(x)$ rises significantly, indicating a decrease in reaction rate and nonlinear effects. This trend highlights the critical role of m in controlling substrate utilization and concentration distribution in catalytic systems.

5.1.4. Effect of n on the concentration The concentration profile $c(x)$ is plotted against the dimensionless distance x for different values of the kinetic parameter n, with $p = 0$, $m = 2$, $\alpha = 0.1$, and $\varphi = 1$ fixed, as shown in Figure(4). The TSM curves closely follow the numerical data points, validating the precision and applicability of the analytical method across varying n. As it n increases from 0 to 20, the concentration $c(x)$ also increases, indicating a weakening of the nonlinearity in the reaction term. This behavior suggests that higher n values lead to slower consumption rates, thereby elevating substrate concentration throughout the domain.

5.1.5. Effect of p on the concentration With $n = 1$, $\alpha = 3.5$, $m = 2$, and $\varphi = 3$ fixed in Figure (5), the role of the convective term p on concentration profiles is evaluated. Increasing p shifts the curves downward, reflecting enhanced transport and reduced substrate retention. The alignment of TSM curves with numerical results underscores the reliability of the analytical method.

5.2. Effectiveness factor (η)

The effectiveness factor (η) has practical implications for catalyst design and operation, suggesting the need for strategies such as reducing particle size or enhancing pore diffusion. As a result, the effectiveness factor η plays a key role in guiding the design and optimization of catalytic systems by assisting in the selection of suitable catalyst shapes and operating parameters, thereby improving overall reaction efficiency and product yield. The trends presented in this study offer actionable insights for catalyst design and scale-up in industrial processes involving porous catalysts with nonlinear reaction kinetics.

Table 6. Effectiveness factor (η) (8) values for various values of φ for $m = 2$, $n = 1$, $p = 0$.

α	$\varphi = 10$ $k = 0.0196$	$\varphi = 20$ $k = 0.0050$	$\varphi = 30$ $k = 0.0022$	$\varphi = 50$ $k = 0.0008$
0	0.0196	0.0050	0.0022	0.0008
10	0.2122	0.0547	0.0244	0.0088
20	0.0539	0.1043	0.0466	0.0168
30	0.0340	0.0439	0.0687	0.0248
40	0.0251	0.0280	0.0909	0.0328
50	0.0200	0.0213	0.0248	0.0408
60	0.0166	0.0173	0.0190	0.0488
70	0.0142	0.0147	0.0156	0.0237
80	0.0124	0.0127	0.0133	0.0164
90	0.0111	0.0113	0.0116	0.0134
100	0.0099	0.0101	0.0104	0.0115

Table 7. Effectiveness factor (η) (8) for various values of α for $m = 2$, $n = 1$, $p = 0$.

φ	$\alpha = 10$ $k = 0.0909$	$\alpha = 20$ $k = 0.0476$	$\alpha = 30$ $k = 0.0323$	$\alpha = 50$ $k = 0.0196$	$\alpha = 100$ $k = 0.0099$
0	0.0909	0.0476	0.0323	0.0196	0.0099
10	0.2122	0.0539	0.0340	0.0200	0.0099
20	0.0547	0.1043	0.0439	0.0213	0.0101
30	0.0244	0.0466	0.0687	0.0248	0.0104
40	0.0137	0.0262	0.0387	0.0637	0.0108
50	0.0088	0.0168	0.0248	0.0408	0.0115
60	0.0061	0.0117	0.0172	0.0283	0.0127
70	0.0045	0.0086	0.0126	0.0208	0.0159
80	0.0034	0.0066	0.0097	0.0159	0.0316
90	0.0027	0.0052	0.0077	0.0126	0.0249
100	0.0022	0.0042	0.0062	0.0102	0.0202

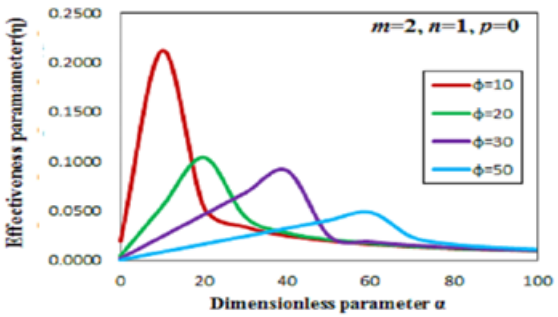

Figure 6. Variation of the effectiveness factor η with the dimensionless parameter α for different values of the Thiele modulus φ ($\varphi = 10, 20, 30, 50$) at fixed parameters $m = 2$, $n = 1$, and $p = 0$.

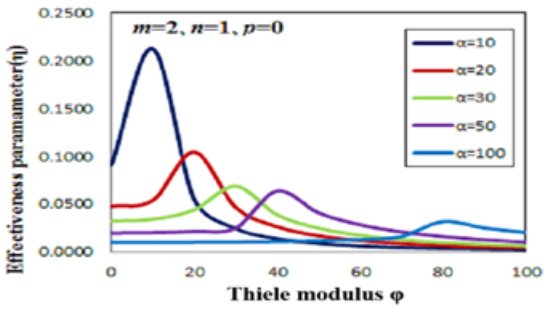

Figure 7. Variation of the effectiveness factor η with the Thiele modulus φ for different values of the dimensionless parameter α ($\alpha = 10, 20, 30, 50, 100$) at fixed parameters $m = 2$, $n = 1$, and $p = 0$.

5.2.1. Impact of φ on the Effectiveness Factor η Figure (6) illustrates the variation of the effectiveness factor (η) with respect to the dimensionless parameter α for different values of the Thiele modulus φ (10, 20, 30, and 50), under fixed conditions: $m = 2$, $n = 1$, and $p = 0$. The plot reveals a non-monotonic trend, where η initially increases with α, reaches a maximum, and then gradually declines as α continues to rise. Higher φ values shift the peak position toward larger α values and lower the peak height, indicating stronger internal diffusion resistance. This behavior highlights the interplay between reaction and diffusion phenomena in porous catalysts and demonstrates how increasing diffusional limitations (i.e., higher φ) reduce the catalyst's overall effectiveness.

5.2.2. Impact of α on Effectiveness factor η Figure (7) displays the influence of the Thiele modulus (φ) on the effectiveness factor (η) for different values of the dimensionless parameter α (10, 20, 30, 50, and 100), with fixed kinetic parameters $m = 2$, $n = 1$, and $p = 0$. Each curve exhibits a distinct peak, indicating an optimal point φ at which it η is maximized for a given α. As it α increases, the peak of η shifts toward higher φ values, while the maximum η decreases, demonstrating the suppressing effect of stronger reaction resistance on catalyst efficiency. This behaviour highlights the complex interplay between reaction kinetics (α) and internal diffusion (φ), showing that both parameters must be carefully balanced to optimize catalyst utilization in porous media.

It is also noted that in Figure (6) and Figure (7), at the beginning, the effectiveness factor increases with increasing α and φ, respectively, and reaches a maximum value for each case. After reaching this maximum, the effectiveness factor decreases, illustrating the non-monotonic relationship between η and both α and φ.

5.3. Analysis of convergence and truncation error of Taylor SeriesMethod(TSM)

The nonlinear ODE was solved analytically using a Taylor series expansion with the parameters $p = 0$, $\alpha = 0.1$, $m = 2, n = 5$, $k = 0.831$, and $\varphi = 1$. The resulting approximate solutions are given by considering 5-term, 6-term, and 7-term expansions:

$$c(x) \approx 0.831 + 0.1688x^2 + 0.0276x^4, \tag{9}$$

$$c(x) \approx 0.831 + 0.1688x^2 + 0.0276x^4 + 0.00425x^6, \tag{10}$$

$$c(x) \approx 0.831 + 0.1688x^2 + 0.0276x^4 + 0.00425x^6 + 0.00368x^7. \tag{11}$$

To assess the accuracy of this truncated series, the residual $R(x)$ was computed as

$$R(x) = \left| c''(x) - pc'(x) - B(c(x)) \right|, \tag{12}$$

with the nonlinear term

$$B(c(x)) \approx \frac{[c(x)]^5}{\left(1 + 0.1\, c(x)\right)^2}.$$

This yields:

$$R_5(x) \approx \left|0.0076 - 0.0028x^2 + 0.0727x^4\right|, \tag{13}$$
$$R_6(x) \approx \left|0.0076 - 0.0028x^2 + 0.0727x^4 - 0.001x^6\right|, \tag{14}$$
$$R_7(x) \approx \left|0.0076 - 0.0028x^2 + 0.0727x^4 - 0.001x^6 + 0.0015x^7\right|. \tag{15}$$

Here, $R_5(x)$, $R_6(x)$, and $R_7(x)$ denote the residuals of the 5-term, 6-term, and 7-term expansions, respectively. The truncation error for c(x) is also estimated using

$$E_n(x) \approx \left|a_{n+1}x^{n+1}\right|, \tag{16}$$

and assuming $x \in [0, 1]$, the maximum truncation error occurs at $x = 1$, yielding

$$E_5^{\max} = 0.00425, \quad E_6^{\max} = 0.00368, \quad E_7^{\max} = 0.002. \tag{17}$$

These results confirm that higher-order contributions rapidly diminish and the truncated solutions remain accurate within the domain. Moreover, the residual error remained below acceptable thresholds, showing that the approximate solutions satisfy the governing ODE to a high degree of accuracy.
Also we find Root Test, $L_n = \sqrt[n]{|a_n|}$,

A convergence analysis via the Root test further established absolute convergence, with representative values

$$L_0 = 0.831, \quad L_2 = 0.411, \quad L_4 = 0.408, \quad L_6 = 0.402, \quad L_7 = 0.449, \quad L_8 = 0.460,$$

all satisfying $L < 1$.

Taken together, the residual analysis, truncation error bounds, and Root Test confirm that the truncated Taylor series expansion provides a convergent and reliable approximation of $c(x)$ across the considered domain.

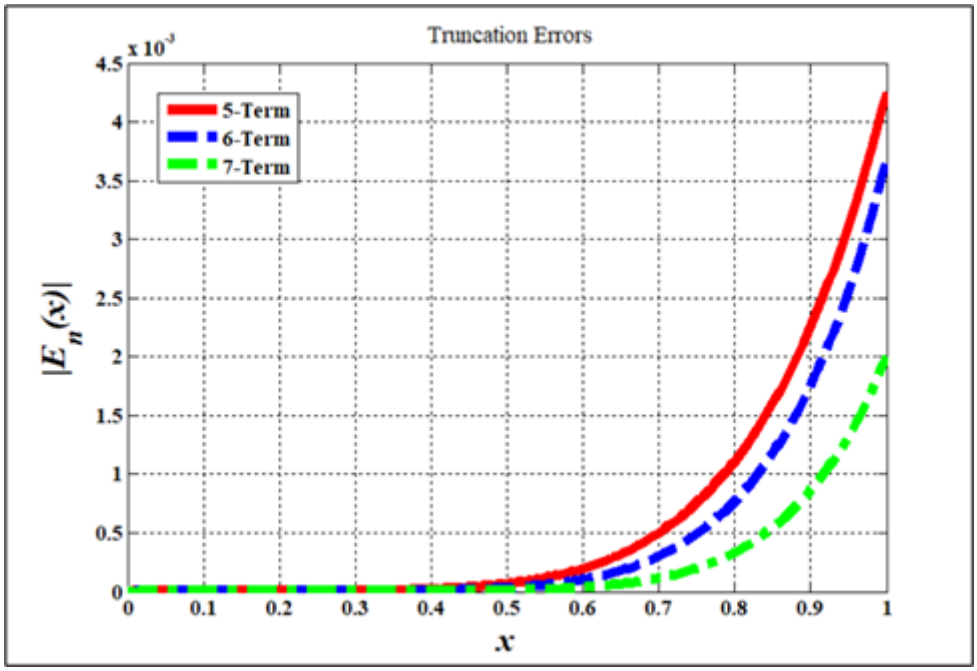

Figure 8. Truncation errors for 5-term, 6-term, and 7-term series approximations as a function of dimensionless distance x. Increasing the number of terms reduces the truncation error significantly, especially for larger values of x when $p = 0$, $\alpha = 0.1$, $m = 2$, $n = 5$, $k = 0.831$, and $\varphi = 1$.

Figure (8) illustrates the truncation errors for the 5-term, 6-term, and 7-term Taylor series approximations of c(x). The error systematically decreases with the inclusion of higher-order terms, with the 7-term expansion yielding the smallest deviation, particularly near x=1. However, the improvement beyond the 5-term approximation is marginal, and since the 5-term series already maintains errors within an acceptable bound across the entire domain, it can be concluded that retaining five terms is sufficient for an accurate representation of the solution.

5.3.1. Perturbation versus Taylor Series Method (TSM) The first-order perturbation solution assumes a small Thiele modulus ($\varphi \ll 1$) and can be expressed as

$$c(x) \approx c_0(x) + \varphi^2 c_1(x) + O(\varphi^4). \tag{18}$$

At zeroth and first order, the governing equations become

$$c_0'' - pc_0' = 0, \tag{19}$$

$$c_1'' - pc_1' = \frac{c_0}{1+\alpha c_0} = \frac{2}{3}. \tag{20}$$

For the case $p = 1$, $\alpha = 0.5$, $m = 1$, $n = 1$, and $\varphi = 0.05$, the solutions are

$$c_0(x) = 1, \quad c_1(x) = -0.457 + 0.667e^x - 0.667x.$$

Thus, the perturbation approximation is

$$c(x) \approx 1 + 0.0025\left[-0.457 + 0.667e^x - 0.667x\right].$$

The final TSM solution obtained from Eq. (7) and the perturbation solution Eq. (18) are summarized in Table 8.

Table 8. Comparison of Perturbation and TSM Results for $p = 1$, $\alpha = 0.5$, $m = 1$, $n = 1$, $\varphi = 0.05$.

Method	**Approximation of** $c(x)$ $(0 \le x \le 1)$	**Accuracy / Remarks**
PerturbationEq. (18)	$c(x) \approx 1 + 0.0025[-0.457 + 0.667e^x - 0.667x]$ $c(x) \approx 0.998857 - 0.0016675e^x - 0.0016675x$	Simple analytical form, good for small φ, slightly less accurate.
TSM(5-term)Eq. (7)	$c(x) \approx 0.9987 + 0.001248x^2 + 0.000416x^3 + 0.000101x^4 + 0.000021x^5$	Excellent agreement with numerical solution; more accurate than first-order perturbation.

The results show that the TSM (5-term Taylor expansion) provides excellent agreement with the numerical solution, while the perturbation method, though simpler, is slightly less accurate. This comparison quantitatively demonstrates the efficiency of TSM relative to a standard analytical method.

The Figure (9)shows a comparison between perturbation, TSM (Taylor Series Method) 5-term, and numerical solutions for the function $c(x)$ over the range of x. The perturbation solution (red line) consistently predicts higher values than both the TSM 5-term (dashed black) and numerical (dash-dot black) solutions. The TSM 5-term and numerical solution curves closely overlap, indicating high accuracy of the truncated Taylor expansion in this range. The differences between methods gradually widen as x increases, highlighting the growing truncation error for series approximations. The figure effectively illustrates the comparative behavior and error propagation among the three approaches across the interval.

5.4. Validation of TSM through comparison with ADM

The Taylor Series Method (TSM) provides an approximate analytical solution for the concentration profile in the considered nonlinear system. To evaluate its accuracy and reliability, TSM is compared with the Adomian

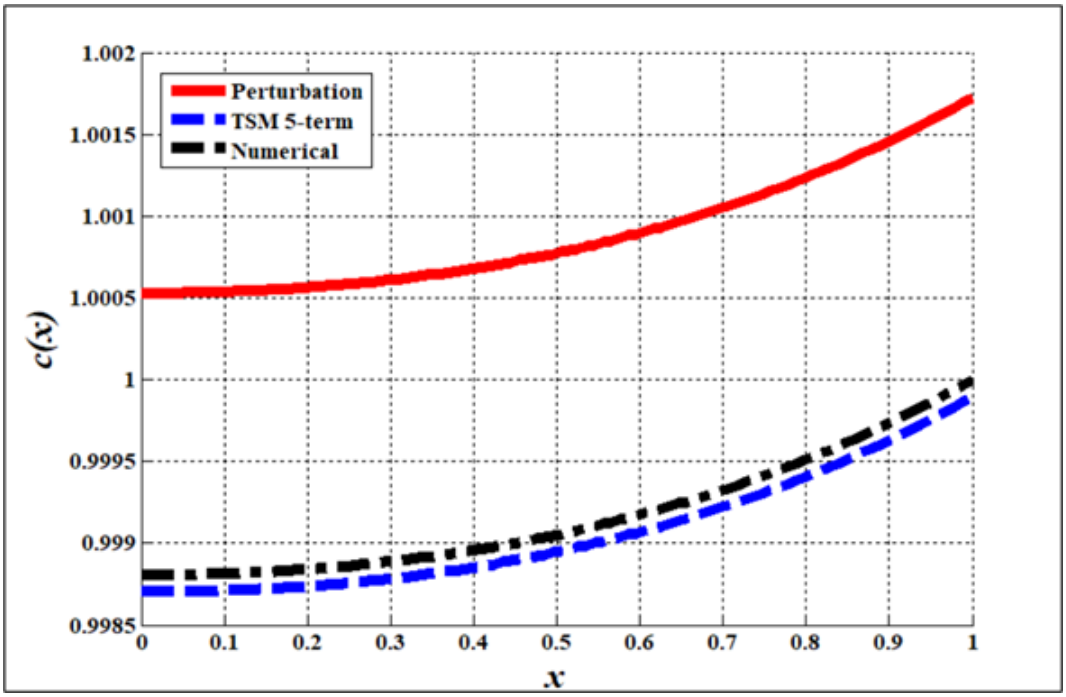

Figure 9. Comparison figure for perturbation and TSM for $p = 1$, $\alpha = 0.5$, $m = 1$, $n = 1$, and $\varphi = 0.05$.

Table 9. Comparison table for TSM Eq. (7) and ADM Eq. (11) for $p = 0$, $m = 3$, $n = 1$, $\alpha = 10$, $\varphi = 2$.

x	TSM (Eq.(7))	ADM (Eq.(11) in [5])	Numerical	Abs. Dev (TSM)	Abs. Dev (ADM)
0.0	0.9985	0.9985	0.9985	0.0000	0.0000
0.1	0.9985	0.9985	0.9985	0.0000	0.0000
0.2	0.9986	0.9986	0.9986	0.0000	0.0000
0.3	0.9986	0.9986	0.9986	0.0000	0.0000
0.4	0.9987	0.9987	0.9987	0.0000	0.0000
0.5	0.9989	0.9989	0.9989	0.0000	0.0000
0.6	0.9991	0.9990	0.9991	0.0000	0.0001
0.7	0.9993	0.9992	0.9993	0.0000	0.0001
0.8	0.9995	0.9995	0.9995	0.0000	0.0000
0.9	0.9997	0.9997	0.9997	0.0000	0.0000
1.0	1.0000	1.0000	1.0000	0.0000	0.0000

Decomposition Method (ADM) and numerical solutions. Such comparison allows us to identify the precision of TSM across the spatial domain and verify its suitability for modeling the system under the chosen parameter regime. This step ensures that subsequent analyses based on TSM are grounded on a validated methodology.

The table presents a comparative analysis of the Taylor Series Method (TSM, Eq. (7)) and the Adomian Decomposition Method (ADM, Eq. (11)) in [5]) for the parameter set $p = 0$, $m = 3$, $n = 1$, $\alpha = 10$, $\varphi = 2$. Both TSM and ADM solutions closely match the numerical results across $x \in [0, 1]$ with negligible absolute deviations. Minor differences between ADM and TSM appear at intermediate points ($x = 0.6$ and 0.7), but TSM shows slightly better agreement with the numerical solution. This indicates that TSM provides a more accurate and reliable approximation of the concentration profile. Overall, TSM is demonstrated to be superior to ADM for this parameter regime.

5.5. Sensitivity analysis of parameters on the effectiveness factor

The sensitivities were evaluated using *local sensitivity analysis*, which quantifies the response of the effectiveness factor η to small perturbations in each parameter. The effectiveness factor is defined in terms of the implicit root k obtained from the boundary condition $c(1) = 1$. For each parameter, central finite differences were applied: the parameter was perturbed by a small relative step, the boundary equation was re-solved to update k, and the resulting change in η was used to compute $\partial\eta/\partial\theta$. These derivatives were then normalized using the dimensionless form

$$S_\theta = \frac{\theta}{\eta}\frac{\partial \eta}{\partial \theta}. \tag{21}$$

Finally, absolute values of S_θ were used to obtain percentage contributions, ensuring comparability of the relative influence of each parameter. This approach captures both the direct dependence of η on the parameters and the indirect effects mediated through the numerical solution for k. Figure 10 illustrates the normalized local sensitivity

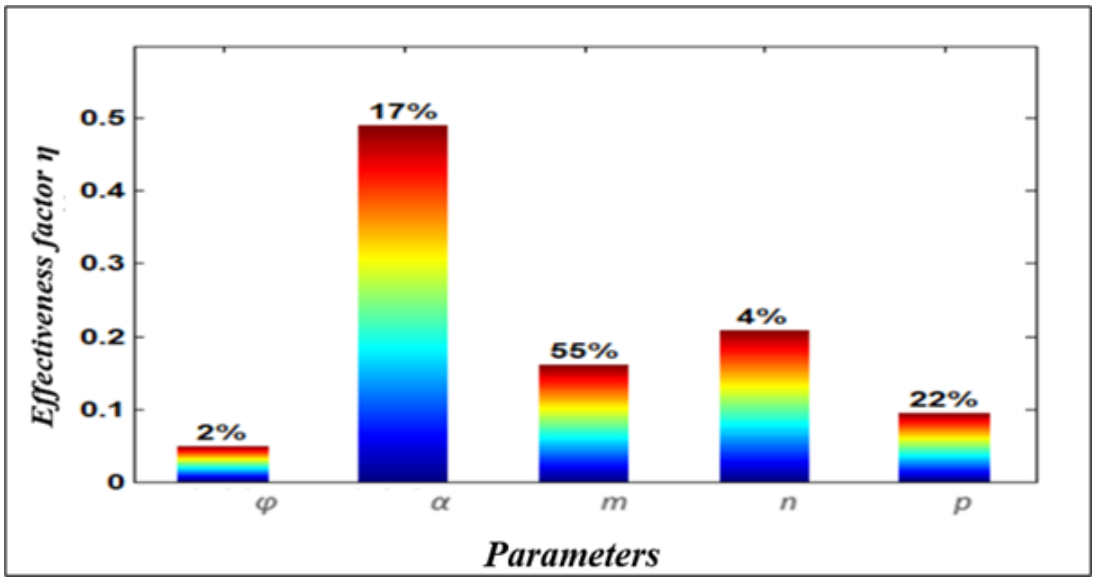

Figure 10. Sensitivity analysis of parameters: Percent change in dimensionless effectiveness factor η for φ =1, α = 2, m =2, n = 1, and p = 2.

indices of the effectiveness factor η with respect to the governing parameters φ, α, m, n, and p. The gradient bar plot highlights the relative contribution of each parameter, expressed in percentages. Among the parameters, the exponent on the denominator (m) shows the highest influence ($\approx 55\%$), indicating its dominant role in controlling η. The convective parameter p also exhibits a strong effect ($\approx 22\%$), followed by the adsorption factor α ($\approx 17\%$). In contrast, the reaction order n ($\approx 4\%$) and Thiele modulus-like term φ ($\approx 2\%$) contribute comparatively less. This ranking clearly demonstrates that while all parameters have some impact, m and p are the most critical in the present regime.

6. Conclusion

We developed a theoretical framework to analyse the coupled effects of reaction and diffusion within porous catalysts, deriving analytical solutions and validating them through numerical comparisons. This combined methodology offered clear insights into how factors like enzyme concentration and buffer composition affect the efficiency of the catalytic system. From a statistical and computational standpoint, our model provides a

basis for predictive analysis and optimization, offering a systematic method to evaluate parameter sensitivities and operational efficiency. Beyond reaction engineering, these findings support the advancement of optimization algorithms and statistical computing methods that rely on robust modeling for better system analysis and decision-making.

Nomenclature

Table 10. List of symbols used in the present study

Symbol	Meaning	Unit
D_{eff}	Effective diffusion coefficient of species A	m^2/s
C_A	Molar concentration of species A	mol/m^3
$(C_A)_s$	Concentration at the external surface of the catalyst	mol/m^3
k_v	Reaction rate constant	$mol^{p-1}\ m^{-3(p-1)}\ s^{-1}$
K_A	Adsorption inhibition constant of species A	m^3/mol
p, m, n	Numerical constants	-
l	Thickness of flat catalyst	m
L_C	Characteristic length	m
R	Radius of the catalyst particle	m
$c(x)$	Dimensionless concentration	-
x	Dimensionless distance	-
Greek letters		
α	Dimensionless parameter	-
φ	Thiele modulus	-
η	Effectiveness parameter	-

Appendix A. Solution of (7) as: by the Taylor Series Method

he nonlinear differential equation is given as

$$c''(x) - p\,c'(x) - B(c) = 0, \quad 0 \le x \le 1, \tag{A1}$$

with the boundary conditions

$$c'(0) = 0, \tag{A2}$$

$$c(1) = 1. \tag{A3}$$

Assuming the solution can be expanded in a Taylor series about $x = 0$, we have

$$c(x) = c(0) + \frac{c'(0)x}{1!} + \frac{c''(0)x^2}{2!} + \frac{c'''(0)x^3}{3!} + \frac{c^{(4)}(0)x^4}{4!} + \frac{c^{(5)}(0)x^5}{5!} + \cdots \tag{A4}$$

From Eq. (A1), we can rewrite

$$c''(x) = p\,c'(x) + B(c), \tag{A5}$$

and recursively obtain higher derivatives

$$\begin{aligned} c'''(x) &= p\,c''(x) + B'(c)\,c'(x), \\ c^{(4)}(x) &= p\,c'''(x) + B'(c)\,c''(x) + B''(c)\,[c'(x)]^2, \\ c^{(5)}(x) &= p\,c^{(4)}(x) + B'(c)\,c'''(x) + 3B''(c)\,c'(x)c''(x) + B'''(c)\,[c'(x)]^3, \end{aligned} \tag{A6}$$

where

$$B(c) = \frac{\varphi^2[c(x)]^n}{[1+\alpha c(x)]^m}, \quad B'(x) = B'(c)\,c'(x), \quad B''(x) = B'(c)\,c''(x) + B''(c)\,[c'(x)]^2, \ldots \tag{A7}$$

Applying the boundary condition $c'(0) = 0$, we have

$$\begin{aligned} c'(0) &= 0, \\ c''(0) &= B(c_0), \\ c'''(0) &= p\,c''(0), \\ c^{(4)}(0) &= p\,c'''(0) + B'(c_0)\,c''(0), \\ c^{(5)}(0) &= p\,c^{(4)}(0) + B'(c_0)\,c'''(0), \end{aligned} \tag{A8}$$

where $c_0 = c(0)$ is unknown.

Thus, the Taylor series solution becomes

$$c(x) = \sum_{q=0}^{\infty} \frac{c^{(q)}(0)}{q!} x^q \tag{A9}$$

and, after simplification, we obtain

$$c(x) = c_0 + \frac{B(c_0)x^2}{2!} + \frac{pB(c_0)x^3}{3!} + \frac{(p^2 + B'(c_0))B(c_0)x^4}{4!} + \frac{p(p^2 + 2B'(c_0))B(c_0)x^5}{5!} \tag{A10}$$

Let $c_0 = k$ and $B(c_0) = \frac{\varphi^2 k^n}{(1+\alpha k)^m}$. Since $B'(c_0) = 0$ due to $c'(0) = 0$, Eq. (A10) reduces to

$$c(x) = k + \frac{(\varphi^2 k^n/(1+\alpha k)^m)x^2}{2!} + \frac{p(\varphi^2 k^n/(1+\alpha k)^m)x^3}{3!} + \frac{p^2(\varphi^2 k^n/(1+\alpha k)^m)x^4}{4!} + \frac{p^3(\varphi^2 k^n/(1+\alpha k)^m)x^5}{5!} + \tag{A11}$$

$$k + \frac{(\varphi^2 k^n/(1+\alpha k)^m)}{2!} + \frac{p(\varphi^2 k^n/(1+\alpha k)^m)}{3!} + \frac{p^2(\varphi^2 k^n/(1+\alpha k)^m)}{4!} + \frac{p^3(\varphi^2 k^n/(1+\alpha k)^m)}{5!} = 1. \tag{A12}$$

By using MAPLE, we can find the value of k by giving the experimental values for the unknown parameters φ, α, m, n, and p. For example.

When $n = 1$, $m = 0$, $\alpha = 0$:

$$\frac{\varphi^2 k^n}{(1+\alpha k)^m} = \varphi^2 k$$

Then

$$k = \frac{1}{1 + \frac{\varphi^2}{2} + \frac{p\varphi^2}{6} + \frac{p^2\varphi^2}{24} + \frac{p^2\varphi^2}{120}} \tag{A13}$$

When $n = 1$, $m = 1$, $\alpha = 1$:

$$\frac{\varphi^2 k^n}{(1+\alpha k)^m} = \frac{\varphi^2 k}{1+k}$$

Then

$$k = \frac{-\varphi^2 S + \sqrt{\varphi^4 S^2 + 4}}{2}, \quad \text{with } S = \frac{1}{2} + \frac{p}{6} + \frac{p^2}{24} + \frac{p^2}{120} \tag{A14}$$

Finally, the effectiveness factor η is defined as

$$\eta = \frac{1+\alpha}{\varphi^2} c'(1), \tag{A15}$$

$$c'(x) = \frac{\varphi^2 k^n}{(1+\alpha k)^m} x + \frac{p(\varphi^2 k^n/(1+\alpha k)^m)x^2}{2} + \frac{p^2(\varphi^2 k^n/(1+\alpha k)^m)x^3}{6} + \frac{p^3(\varphi^2 k^n/(1+\alpha k)^m)x^4}{24},$$

$$\eta = \frac{(1+\alpha)k^n}{(1+\alpha k)^m}\left(1 + \frac{p}{2} + \frac{p^2}{6} + \frac{p^3}{24}\right). \tag{A16}$$

The value of k can be obtained numerically using software such as MATLAB or Wolfram Alpha for given experimental values of φ, α, m, n, and p. Also the Ying Buzu algorithm [14], an ancient Chinese root-finding technique [15] also called double false position, iteratively estimates roots by linear interpolation between points of opposite signs. For nonlinear equations with possible multiple roots, combining Ying Buzu with derivative-based methods like Newton's or modified Newton's enhances convergence speed and stability. Software like MAPLE or WolframAlpha.com employs hybrid algorithms that bracket roots first, then refine them. Special techniques, such as deflation handle multiple roots effectively, improving numerical stability and convergence.

Appendix B. MATLAB code for solving a nonlinear boundary value problem

```
function bvp4c
    p = 1;
    phi = 0.05;
    n = 1;
    alpha = 0.5;
    m = 1;
    xspan = [0 1];
    solinit = bvpinit(linspace(0,1,10), [0 1]);
    sol = bvp4c(@(x,c) odefun(x,c,p,phi,n,alpha,m), @bcfun, solinit);
    x = linspace(0,1,100);
    c = deval(sol, x);
    plot(x, c(1,:));
    xlabel('x');
    ylabel('c(x)');
    title('Solution of the non-linear differential equation');
end

function dydx = odefun(x,c,p,phi,n,alpha,m)
    % Define the system of ODEs based on the given differential equation
    dydx = [c(2);
            p * c(2) + (phi^2 * c(1)^n) / (1 + alpha * c(1))^m];
end

function res = bcfun(c0,c1)
    % Boundary conditions
    res = [c0(2);       % At x=0, dc/dx = 0
           c1(1) - 1]; % At x=1, c(1) = 1
end
```

REFERENCES

1. D. Leung, R.E. Hayes, and S.T. Kolaczkowski, *Diffusion limitation effects in the washcoat of a catalytic monolith reactor*, Can. J. Chem. Eng, 74, 94–103, 1996.
2. R.E. Hayes, and S.T. Kolaczkowski, *Mass and heat transfer effects in catalytic monolith reactors* , Chem. Eng. Sci, 49, 3587–3599, 1994.
3. M. Mary, L. Muthusubramanian, P. Jeyabarathi, L. Rajendran , *Effectiveness factor for general porous catalytic particle in Langmuir-Hinshelwood kinetics for isothermal and non-isothermal reactions* , 138, 2535–2552, 2025.
4. M Karthiyayini, P Jeyabarathi, L Rajendran *Theoretical analysis of Langmuir-Hinshelwood kinetics: Hyperbolic function and Akbari–Ganji's method*, Reaction Kinetics, Mechanisms and Catalysis, 138, 1221-1239, 2025.
5. M.K. Sivasankari, and L. Rajendran , *Analytical expression of the concentration of species and effectiveness factors in porous catalysts using the Adomian decomposition method*, Kinet. Catal, 54(1), 95–105, 2013.
6. R.E. Hayes, and M. Votsmeier , *A fast approximation method for computing effectiveness factors with non-linear kinetics* , Chem. Eng. Sci, 62, 2209–2215, 2007.
7. H. Vazquez-Leal, B. Benhammouda, and U.A. *Filobello-Nino, et al* , *Modified Taylor series method for solving nonlinear differential equations with mixed boundary conditions defined on finite intervals* , SpringerPlus, 3, 160, 2014.
8. Y.P. Sun, S.B. Liu, and S. Keith , *Approximate solution for the nonlinear model of diffusion and reaction in porous catalysts by the decomposition method* , *Chem. Eng.* J, 102(1), 1–10, 2004 .
9. A.J. Ellery, and M.J. Simpson , *An analytical method to solve a general class of nonlinear reactive transport models* , Chem. Eng. J, 169(1-3), 313–318, 2011 .
10. S. Abbasbandy, and M.T. Darvishi, *A numerical solution of Burgers' equation by modified Adomian method*, Appl. Math. Comput, 163, 1265–1275, 2005 .
11. R.K. Bhattacharyya, and R.K. Bera , *Application of Adomian method on the solution of the elastic wave propagation in elastic bars of finite length with randomly and linearly varying young's modulus* , Appl. Math. Lett., 17, 703–709, 2004 .
12. S.M. El Sayed, and D. Kaya , *On the numerical solution of the system of two-dimensional Burgers' equations by the decomposition method* , Appl. Math. Comput, 158, 101–110, 2004 .
13. S. Guellal, P. Grimalt, Y. Cherruault , *Numerical study of Lorenz's equation by the Adomian method* , Comput. Math. Appl., 33, 25–29, 1997 .
14. K. Lakshmi Narayanan, R. Shanthi, R. Ramu Usha Rani, Michael E.G. Lyons, and Lakshmanan Rajendran, *Mathematical modelling of forced convection in a porous medium for a general geometry: Solution of thermal energy equation via Taylor's series with Ying Buzu algorithms*, *Int. J. Electrochem. Sci.*, 17, Article 220623, 2022.
15. Hung-Hua Sheu, Tzu-Te Lin, and Ming-Der Ger, *Effect of ammonium formate addition on corrosion behavior of trivalent chromium coatings electrodeposited in deep eutectic solvents*, *Int. J. Electrochem. Sci.*, 17, Article 22076, 2022.